Turbine Combustor Preliminary Design Approach

A. M. Mellor* and K. J. Fritsky†
Drexel University, Philadelphia, Pennsylvania 19104

Semiempirical correlations calibrated with data from a wide variety of existing gas turbine combustors are rearranged and organized into a burner design methodology, yielding position and size of primary and secondary air penetration holes and swirler angle, as well as required atomization from both pilot and main fuel injectors at engine start and low power operating conditions. The methodology assumes the design fuel has been chosen and that combustor inlet conditions, overall length, and diameter (or annulus height) are known from mission and engine cycle analyses. Output parameters are based on quantitative specifications of maximum NO_x and CO emissions indices, maximum blowout fuel/air ratio at start and idle power, minimum combustion efficiency, and coldest fuel temperature at start (ground or at altitude). Insofar as possible, the methodology is verified with measurements for the three configurations of a can combustor developed for vehicular applications.

Nomenclature

A_{comb} = combustor cross-sectional area
A_{dome} = dome airflow area
A_{pz} = primary hole and dome airflow area
A_{sec} = secondary hole area
A_{tot} = total area through which air enters combustor
b = intercept of a linear equation; preexponential factor
CO = carbon monoxide
c_{pa} = constant pressure specific heat of air at 1300 K
DF-1 = Diesel fuel number one
DF-2 = Diesel fuel number two
d_{comb} = combustor diameter (annulus height)
d_{dome} = dome air hole diameter
d_{film} = film cooling slot height
d_{pri} = primary air penetration hole diameter
d_q = ignition length scale Eq. (6)
d_{sec} = secondary air penetration hole diameter
E = activation energy
E_{gap} = rated energy at ignitor gap
EI = emissions index
FAR = fuel-air ratio
HC = unburned hydrocarbons
k = see Eq. (3)
LHS = left-hand side
l_{co} = characteristic length for lean blowoff, CO emissions, and combustion efficiency in characteristic time models
l_{comb} = combustor length
l_{dome} = average dome air length
l_{film} = film cooling length—distance downstream from fuel injector tip to trailing edge of film cooling slot
l_{no} = characteristic length for NO_x emissions
l_{pri} = primary length—distance downstream from fuel injector tip to centerline of first row of air addition holes
l_{quench} = quench length—distance downstream from fuel injector tip to quench location
l_{sec} = secondary length—distance downstream from fuel injector tip to centerline of second row of air addition holes
m = slope of a linear equation
$\dot{m}_a$ = combustor airflow rate
$(\dot{m}_{apz}/\dot{m}_a)$ = fraction of airflow in primary zone
NO_x = oxides of nitrogen
Nu = Nusselt number
n_{pri} = number of primary air jets
n_{sec} = number of secondary air jets
P_{in} = combustor inlet air pressure
R = universal gas constant; correlation coefficient
RHS = right-hand side
SMD = Sauter mean diameter
$\overline{T}$ = average of burner inlet and outlet temperatures
T_{in} = combustor inlet air temperature
T_{out} = burner outlet temperature
$T_{\phi=1}$ = adiabatic stoichiometric flame temperature
T_η = weighted average of burner inlet and outlet temperatures
V_{ref} = reference velocity—velocity of airflow at maximum combustor cross-sectional area
$V_{\phi=1}$ = stoichiometric flame zone velocity
β = convective evaporation coefficient in d^2 law
β_0 = angle of air injection measured perpendicular to combustor centerline
Δd = liner diameter or annulus height
ΔP_{comb} = liner pressure drop
ΔP_{diff} = diffuser pressure drop
$\Delta T_{\phi=1}$ = temperature rise from inlet temperature to adiabatic stoichiometric flame temperature
ϕ = equivalence ratio
ϕ_{pz} = primary zone equivalence ratio
η = combustion efficiency
θ = swirl angle
ρ_a = density of air at 1300 K
τ_{co} = characteristic time for CO oxidation
τ_{eb} = characteristic time for fuel droplet evaporation,
τ'_{eb} = $(T_{\phi=1}/T_{in})\tau_{eb}$
τ_{hc} = characteristic time for chemical kinetics,
τ'_{hc} = $(T_{\phi=1}/T_{in})\tau_{hc}$
τ_{no} = characteristic kinetics time for NO_x formation
$\tau_{sl,co}$ = residence time in initial shear layer
$\tau_{sl,no}$ = residence time in final, near stoichiometric shear layer
τ_{sl} = shear layer or ignitor residence time
τ_η = characteristic time for CO and hydrocarbon kinetics
τ^*_η = modified combustion efficiency kinetic time

Received Jan. 14, 1989; revision received April 15, 1989.

*Hess Chair Professor of Combustion, Department of Mechanical Engineering and Mechanics; currently Centennial Professor of Mechanical Engineering, Vanderbilt University, Nashville, TN. Member AIAA.

†Undergraduate and NSF Summer Student, Department of Mechanical Engineering and Mechanics.

Introduction

WITH the imposition of more rigorous design performance goals and the eventual use of alternative fuels in gas turbine engine combustors, analytical methods are needed to assist in designing combustors which will satisfy these requirements. For example, in Table 1, Dodds and Ekstedt[1] cite several customer design criteria to be met as part of the NASA Broad Specification Fuels effort, which included goals for performance characteristics such as combustion efficiency, pollutant emissions (CO, HC, NO_x), soot formation (or smoke), profile and pattern factors, blowout fuel-air ratio at idle, and altitude relight. The characteristic time model[2] can be used for achieving efficiency, emissions, ignition, and flame stability goals but does not address liner metal temperatures, smoke levels, and profile/pattern factors, all of which can be treated with correlations from Lefebvre[3] if suitable constants are known. These constants must be obtained by correlating data for a combustor similar to the new preliminary design. An alternative approach is the use of multidimensional computations from a three-dimensional code along with Lefebvre's semiempirical correlations, a hybrid method presented by Rizk and Mongia.[4,5]

Combustor Design Methodology

Here a method for implementing the characteristic time models (CTM) in the combustor design process will be discussed. This method is presented through the use of flowcharts which specify information required as input as well as output to achieve certain performance and emissions goals. A schematic overview of this methodology is presented in Fig. 1. Information made available to the combustor designer as a result of customer specifications and engine cycle requirements is shown in boxes at the left side of the figure. This information coupled with the characteristic time models for emissions, efficiency, lean blowout, and ignition serves as the foundation for specifying design features such as primary and dilution air addition hole locations, diameters, and numbers, swirl angle, and spray Sauter mean diameters (SMD) at start and idle. These design features are shown at the right side of Fig. 1.

Table 1 Performance and Emissions Goals (Ref. 1)

- Combustion efficiency, as computed from emissions measurements, greater than 99% at all operating conditions
- Total pressure loss no more than 6% at sea-level takeoff conditions (Design value = 4.7%)
- Combustor-exit-temperature pattern factor $(T_{4max} - T_{4ave})/(T_{4ave} - T_3)$ no more than 0.25 at sea-level takeoff conditions
  T_3 = average measured total temperature at combustor inlet
  T_{4ave} = average measured total temperature at combustor exit
  T_{4max} = maximum individual measured total temperature at combustor exit
- Combustor-exit average radial temperature profile factor $(T_{4peak} - T_{4ave})/(T_{4ave} - T_3)$ no more than 0.11 at sea-level takeoff conditions
  T_{4peak} = maximum temperature in average radial profile
- Idle blowout fuel/air ratio no more than 7.5 g/kg
- Altitude relight capability up to 9.14 km
- Carbon-free operation
- No significant resonance within flight envelope

	For single-annular combustor[a]	For advanced combustor concepts
HC, g/kN	6.7	3.0
CO, g/kN	36.1	25.0
NO_x, g/kN	35.3[b]	33.0
Smoke number	19.2	19.2

[a]Currently used on CF6-80A production engine.
[b]Although no NO_x requirement was specified for engines manufactured prior to 1/1/84, this goal was included to provide NO_x technology for engines manufactured after that date.

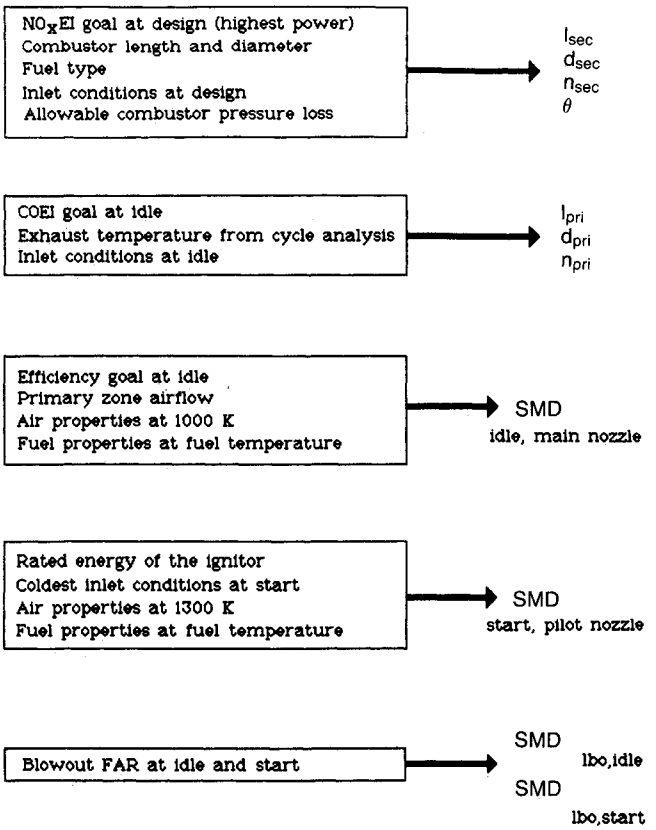

Fig. 1 Schematic overview of gas turbine combustor design methodology. Inputs are at left with outputs at right. Not shown is a possible iteration for SMD_{idle} between blowout and efficiency models (similar to that shown for SMD_{start}).

Figure 2 shows the NO_x emissions flowchart which determines the diameter d_{sec}, number n_{sec}, and downstream distance from fuel injector tip to the centerline of secondary air addition holes l_{sec} for a given emissions index goal at peak NO_x operating conditions (i.e., high power). Other outputs include the total area through which air enters the combustor A_{tot} and swirl angle θ. The inputs required for carrying out the procedure outlined in the flowchart include: the NO_x emissions index goal at design (highest power), the liner diameter(s) Δd and length l_{comb}, the design fuel type, inlet conditions at design, the allowable combustor pressure loss, and known diffuser pressure differential.

The block in the upper right of Fig. 2 contains the characteristic time model equation for NO_x emissions index.[6] Here activation energy E = 135 kcal/g mole and the preexponential factor is in milliseconds. The slope m_{no} and y-intercept b_{no} are included to show the model's dependence on correlated engine data. Mellor and Washam[6] recommended that $m_{no} = 4.5$ and $b_{no} = 0.0$ based on their correlation of NO_x EI (gram NO as NO_2/kg fuel) for the T-63, GT-309, and JT9D engines. If the combustor to be designed using the methodology is a modified version of an existing combustor, then m_{no} and b_{no} could be refined by correlating data specific to that combustor.

The block also contains the variable $V_{\phi=1}$ which is computed from

$$V_{\phi=1} = \frac{\dot{m}_{apz}}{\dot{m}} \frac{T_{\phi=1}}{T_{in}} V_{ref} \tag{1}$$

and for which three quantities must be determined: V_{ref}, $T_{\phi=1}$,

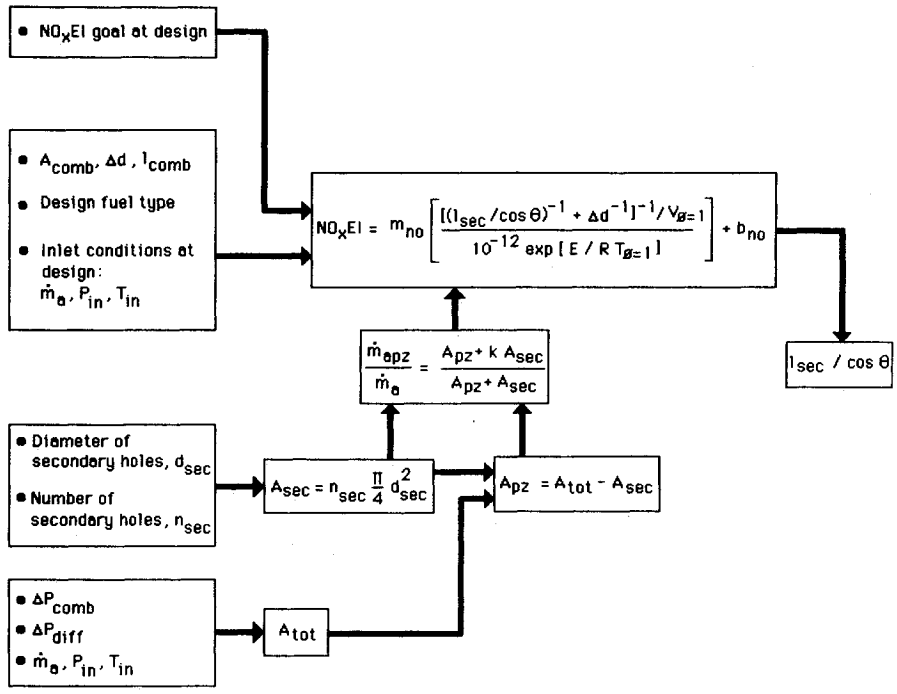

Fig. 2 NO_x emissions flowchart. Parameters in boxes are input, d_{sec} and n_{sec} are first choices in the design process with their final values chosen based on both NO_x and CO emissions flowcharts (see text).

and $\dot{m}_{apz}/\dot{m}_a$. V_{ref} is reference velocity based on combustor cross-sectional area and compressor discharge conditions. $T_{\phi=1}$ is computed from inlet conditions and fuel type.

The $\dot{m}_{apz}/\dot{m}_a$ term is approximated from the ratio of liner areas allotted for primary zone air to total hole area[6] and is estimated as follows. Lefebvre[7] provides an equation for computing the total hole area from combustor pressure loss, diffuser pressure differential, and inlet conditions:

$$A_{tot} = \dot{m}_a \{ [RT_{in}]/[2P_{in}(\Delta P_{comb} - \Delta P_{diff})] \}^{0.5} \quad (2)$$

The secondary hole area A_{sec} is determined from d_{sec} and n_{sec} as shown in Fig. 2. The A_{pz} is found by subtracting A_{sec} from A_{tot}. The liner area allotted for primary zone air ($A_{pz} + kA_{sec}$), is approximated from the sum of the area upstream of the secondary holes A_{pz} and the area through which recirculating dilution air enters the primary zone. This latter area is a fraction of the secondary hole area k computed from

$$k = 0.5(T_{in}/T_{\phi=1})^{0.5} \cos\beta_0 \quad (3)$$

With $\dot{m}_{apz}/\dot{m}_a$ calculated, the quantity $l_{sec}/\cos\theta$ is left as sole output from the model equation. A swirler angle would be chosen (if appropriate for the design) in order to determine l_{sec}. If this value for l_{sec} is greater than the overall length of the combustor l_{comb}, the designer would then increase the diameter and/or the number of secondary holes until a more reasonable l_{sec} is established.

The CO emissions flowchart, as shown in Fig. 3, establishes the location (l_{pri}), diameter (d_{pri}), and number (n_{pri}) of primary air addition holes for a given emissions index goal at peak-CO operating conditions (i.e., low power or idle). Inputs include the CO emissions index goal at idle, the liner diameter(s) and cross-sectional area, the burner outlet temperature determined from cycle analysis, inlet conditions at idle, and swirler angle from the NO_x results. With these inputs established, the equation that predicts CO *EI* is used to determine the quantity $l_{pri}/\cos\theta$. This equation, as shown near the top of Fig. 3, is also taken from Mellor and Washam.[6] Here $\underline{E} = 10.76$ kcal/g mole, the numerator is in milliseconds, and $\overline{T}$ is the average of

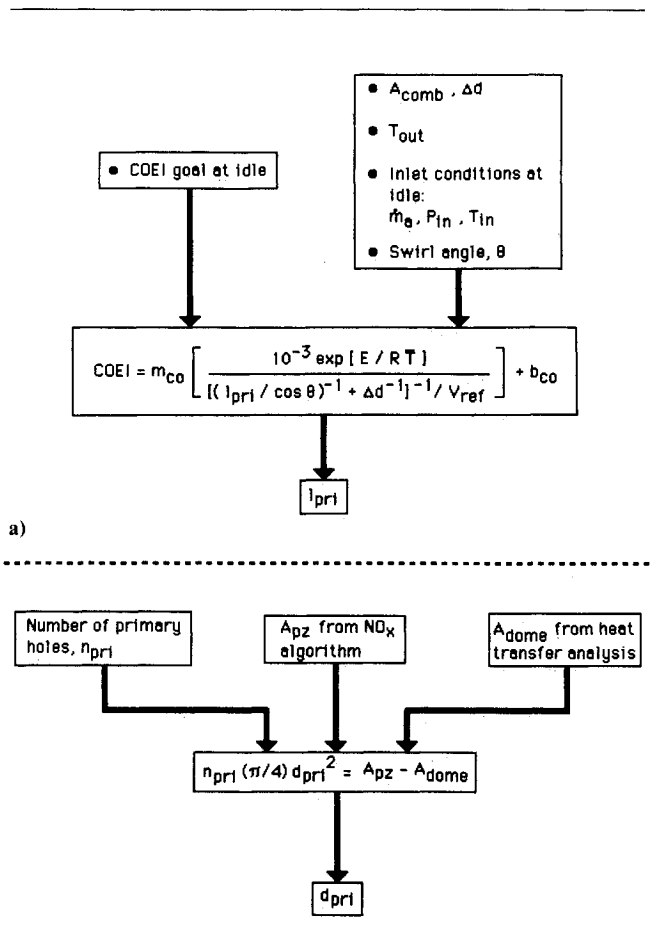

Fig. 3 a) CO emissions flowchart. b) d_{pri} calculation for initial choice of n_{pri}. See text for comparisons of l_{pri} with l_{sec} and l_{film} for possible iterations within CO or with NO emissions flowcharts.

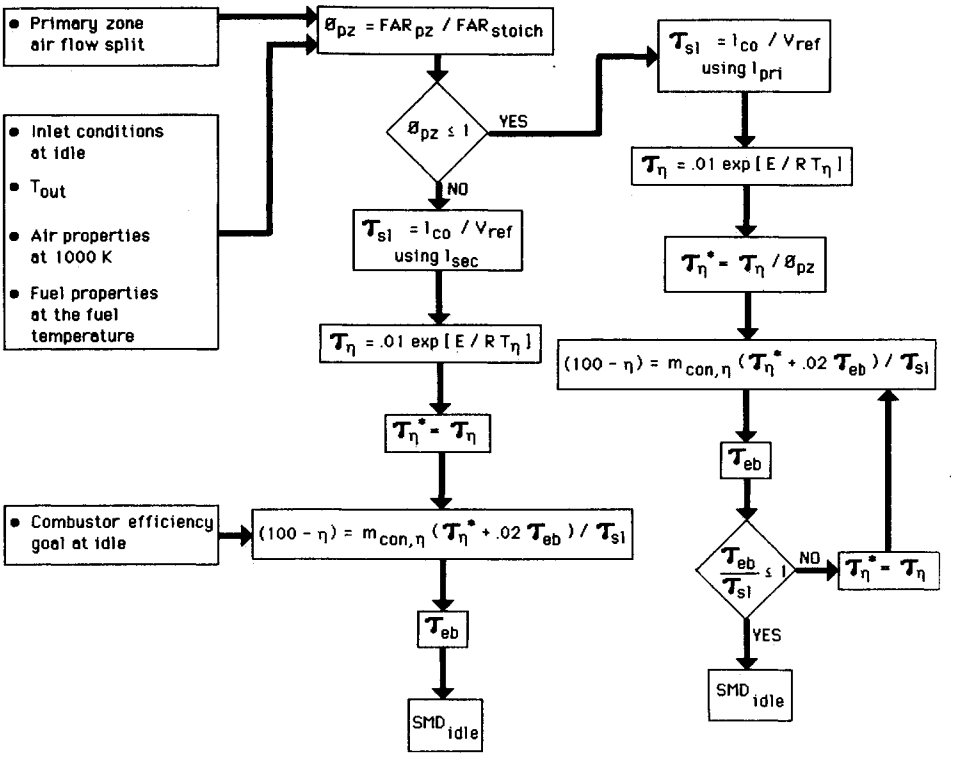

Fig. 4 Combustion efficiency flowchart. An iteration is required between SMD's calculated from the model and that value used initially in the Nusselt number convective correlation in τ_{eb} (see text). Depending on calculated SMD's, iterations may also be required between the combustion efficiency, spark ignition, and lean flame stabilization flowcharts, as discussed in the text.

burner inlet and outlet temperatures, 0.5 ($T_{in} + T_{out}$). As in the NO_x model, the m_{co} and b_{co} terms reflect the model's reliance on actual combustor test data. Mellor and Washam[6] recommend that $m_{co} = 35$ and $b_{co} = 0.0$ as a result of their CO *EI* correlation with the same combustors used for NO_x. If the design includes an air swirler, the swirl angle chosen in the NO_x model would be used to determine l_{pri} from $l_{pri}/\cos\theta$. This length is then compared to l_{sec} to check that first, l_{pri} is less than l_{sec} and second, the distance between the primary and secondary air jets is reasonable with respect to past designs. If the relationship between l_{pri} and l_{sec} is inappropriate, changes are required in the input section of the NO_x algorithm in the form of a different diameter and/or number of secondary holes.

Figure 3 also shows a method for determining d_{pri} and n_{pri}. The liner surface area taken up by primary holes consists of the primary zone area A_{pz} ($= A_{tot} - A_{sec}$) with the exception of flow area associated with the dome and upstream film-cooling slots A_{dome}, which is assumed known from past designs or heat-transfer analysis of the components in this high-temperature region of the combustor. Setting the quantity $[n_{pri}(\pi/4)d_{pri}^2]$ equal to $(A_{pz} - A_{dome})$ allows the designer to obtain a tentative choice for the number and diameter of primary holes.

Figure 4 shows the efficiency flowchart, which establishes a Sauter mean diameter (SMD) and subsequently a main atomizer design in order to achieve a particular combustor efficiency goal at the lowest efficiency operating conditions (i.e., idle), given the combustor geometry chosen in order to meet the NO_x *EI* and CO *EI* goals. This is accomplished by calculating the mean spray droplet evaporation lifetime τ_{eb} from the consecutive process model equation of Leonard[8] shown in the flowchart, which contains two other times, a chemical kinetics time for efficiency τ_η and the initial shear layer mixing time τ_{sl}. In this equation, the intercept term b is set at zero, although Leonard obtained -0.34 with four engines (F101, TF-41, T-63, and AGT-1500). This same correlation gives a recommended value of 3.38 for the slope term, $m_{con,\eta}$ with $E = 4.5$ kcal/g mole for $T_\eta = (0.9T_{in} + 0.1T_{out})$. The inputs to this algorithm include the combustor efficiency goal at idle, the primary zone airflow split approximated from the ratio A_{pz}/A_{tot}, inlet conditions at idle (fuel flow, airflow, inlet air pressure and temperature), the burner outlet temperature determined from cycle analysis, air properties at 1000 K, fuel properties at the fuel temperature, and either l_{pri} or l_{sec}.

The primary zone airflow split is used to compute the primary zone equivalence ratio ϕ_{pz}. Two possible situations arise depending on whether ϕ_{pz} is greater or less than 1. If $\phi_{pz} > 1.0$, then l_{sec} (obtained from the NO_x model) is used in the τ_{sl} computation, where l_{co} in general = (l_{pri} or $l_{sec} + \Delta d^{-1})^{-1}$, and $\tau_\eta^* = \tau_\eta$. At this point a value for τ_{eb} can be determined from τ_{sl}, τ_η^*, and the efficiency goal. If $\phi_{pz} \leq 1.0$, then l_{pri} (obtained from the CO model) is used in the τ_{sl} computation, and it is assumed that $\tau_\eta^* = \tau_\eta/\phi_{pz}$. τ_{eb} is calculated using this assumed value for τ_η^*. In this case, the value of τ_{eb}/τ_{sl} must be ascertained to confirm the use of ϕ_{pz} in τ_η^*. If $\tau_{eb}/\tau_{sl} \leq 1.0$, then the assumption that $\tau_\eta^* = \tau_\eta/\phi_{pz}$ is correct, and τ_{eb} has been determined; if $\tau_{eb}/\tau_{sl} > 1.0$, $\tau_\eta^* = \tau_\eta$ is the recommended value. The redefined τ_η^*, τ_{sl} and the efficiency goal are used to determine τ_{eb}.

The mean spray droplet lifetime τ_{eb} is defined in terms of the SMD and β, the evaporation coefficient based on air properties at 1000 K and modified for forced convection (see Leonard and Mellor[9]) through the d^2 law of Godsave[10]:

$$\tau_{eb} = \text{SMD}^2/\beta \tag{4}$$

Thus, SMD for a specific efficiency goal can be computed knowing τ_{eb} and the evaporation coefficient. Assuming the atomizer is operating with the main nozzle only, a design can now be selected which will deliver the specified fuel flow and produce a spray with the SMD obtained from the algorithm output. At this point, a characteristic SMD vs fuel flow curve

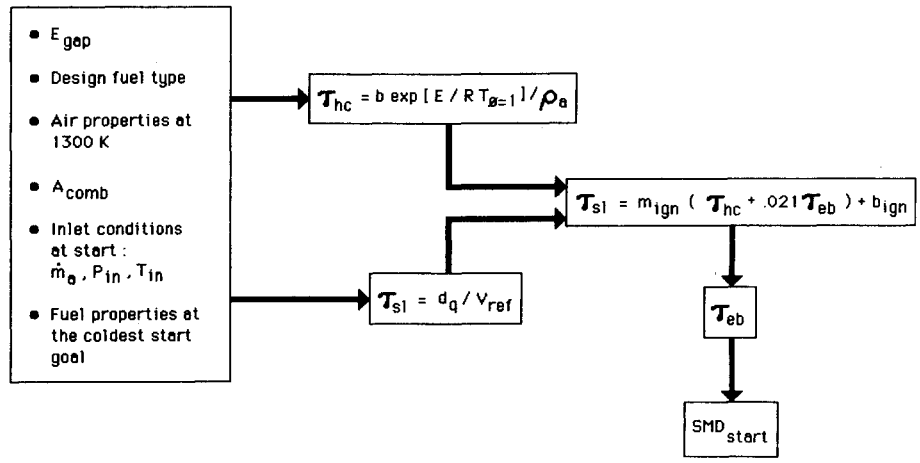

Fig. 5 Spark ignition flowchart. An iteration is required between SMD's calculated from the model and that value used initially in the Nusselt number convective correlation in τ_{eb} (see text). Depending on calculated SMD's, iterations may also be required between the combustion efficiency, spark ignition, and lean flame stabilization flowcharts, as discussed in the text.

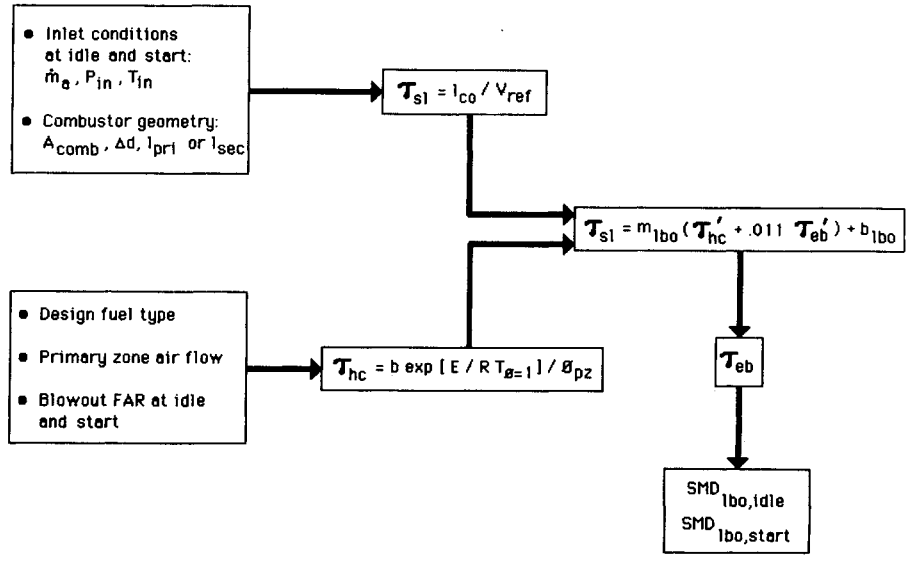

Fig. 6 Lean flame stabilization flowchart. An iteration is required between SMD's calculated from the model and that value used initially in the Nusselt number convective correlation in τ_{eb} (see text). Depending on calculated SMD's, iterations may also be required between the combustion efficiency, spark ignition, and lean flame stabilization flowcharts, as discussed in the text.

is chosen for a main nozzle design based on the known injector fuel flow schedule.

To find a pilot injector SMD value, the cold start ignition criterion (either on the ground or at altitude) is used in conjunction with the spark ignition characteristic time model as shown in Fig. 5. Pilot spray drop lifetime τ_{eb} is calculated from Peters and Mellor's[11] equation for the ignition limit, which requires that the appropriate τ_{sl} and τ_{hc} be known. Here

$$\tau_{sl} = d_q / V_{ref} \tag{5}$$

where the length scale for ignition d_q is taken as the diameter of the small volume of air and fuel vapor heated to $T_{\phi=1}$ by the energy delivered at the spark gap, E_{gap}:

$$d_q = [E_{gap}/(\pi/6)\rho_a c_{pa}(T_{\phi=1} - T_{in})]^{1/3} \tag{6}$$

where air properties in d_q, and for β in τ_{eb}, are evaluated at 1300 K. The fuel vapor ignition delay time τ_{hc} defined in Fig. 5 has $b = 10^{-5}$ kg ms/m^3 and $E = 26.1$ kcal/g mole.

Jarymowycz and Mellor[12] have discussed the appropriate choices for m_{ign} and b_{ign}. Moses et al.[13] found no single values could simultaneously correlate cold start and altitude relight data for 12 different engines, and accordingly ignition tests with early designs of the combustor under study are recommended to refine the model equation in Fig. 5. To start, and here following the Peters and Mellor[14] correlation for the T-63, AGT-1500, and F101 engines, m_{ign} is taken as 1.87 and $b_{ign} = 0.135$.

The following inputs are required in order to compute τ_{sl} and τ_{hc}: the rated energy of the ignitor E_{gap}, the fuel type, air properties at 1300 K, the coldest inlet conditions at start, and fuel properties at the fuel temperature. If the combustor is designed for aircraft applications, inlet air pressure P_{in} is a function of altitude due to static pressure changes. Values for τ_{sl} and τ_{hc} can then be computed as above, and the recommended equation for ignition yields τ_{eb} for the pilot nozzle. With τ_{eb} established and β computed following Peters and Mellor,[11] the SMD required for ignition can be calculated. Assuming the atomizer is operating on pilot only at start, a design can now be selected which will produce a spray with the SMD obtained from the ignition model. For example, for a pressure atomizer, the characteristic SMD specifies an injector flow number. Should this require too high a fuel injection

pressure, then an ignitor delivering a larger energy to the spark gap could be substituted in the ignition algorithm and the process repeated.

The lean blowoff flowchart, shown in Fig. 6, serves to either validate or reject the dual, pilot-main atomizer design chosen using the efficiency and ignition models. A design becomes acceptable when the pilot and main injectors produce with suitable margin a stable flame at start and idle, respectively, for a given blowout fuel-air ratio (*FAR*) goal. The first step in accomplishing this check is to compute two SMD values from the lean blowoff correlation for the blowout *FAR* goal at idle and start. These two values, $SMD_{1bo,idle}$ and $SMD_{1bo,start}$, represent the maximum spray Sauter mean diameters allowable in order to maintain stable combustion.

The inputs to the lean blowoff correlation include the blowout *FAR* at idle and start, inlet conditions at idle and start, the fuel type, and other design features computed previously, including l_{pri} or l_{sec}. The method for deciding which length to use to calculate τ_{sl} begins by assuming that l_{pri} is the correct value. τ_{sl} is calculated as in the efficiency model and τ_{hc} with Eq. (7):

$$\tau_{hc} = 10^{-4} \exp(E/RT_{\phi=1})/\phi_{pz} \text{ (ms)} \quad (7)$$

where $E = 21$ kcal/g mole. The resulting τ_{sl} value, τ_{hc}, and the lean blowoff equation are used to find τ_{eb}. Derr and Mellor[15] recommended that $m_{1bo} = 1.36$ and $b_{1bo} = 0.36$ based on a correlation of the J85, AGT-1500, and T-63 combustors. If $\tau_{eb}/\tau_{sl} < 50.0$, then the assumption that l_{pri} is the correct value is true and τ_{sl} has been determined; otherwise l_{sec} is used to determine τ_{sl}.

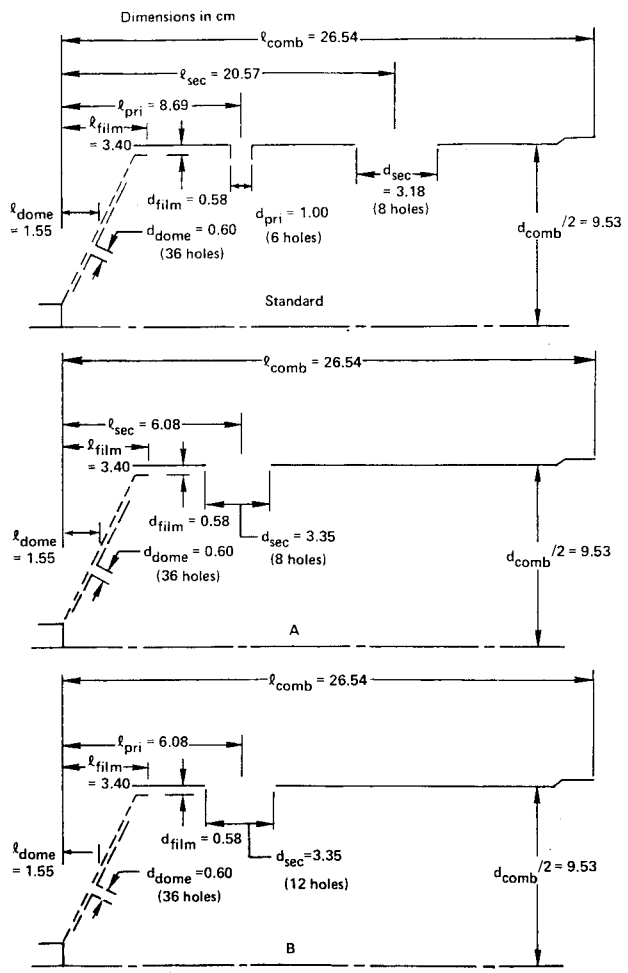

Fig. 7 Geometries for standard, modification A, and modification B GT-309 combustors (Ref. 17).

Table 2 GT-309 engine combustor operating conditions (Ref. 17)

Gasifier shaft speed, % of design	Inlet temperature, K	Inlet pressure, kPa	Air mass flow rate, kg/s	Fuel mass flow rate, kg/h
50	791	146	0.559	6.1
60	757	172	0.726	10.3
70	986	210	0.813	21.0
80	941	255	1.01	31.3
90	897	311	1.25	45.0
100	862	372	1.49	59.8

Using the SMD vs fuel flow curve for the preliminary pilot nozzle design, an SMD for the blowout fuel flow, SMD_{pilot}, can be found and compared to $SMD_{1bo,start}$. If $SMD_{pilot} < SMD_{1bo,start}$, then the pilot nozzle design is acceptable. If unacceptable, then two possible remedies must be investigated. First, new nozzle flow numbers could be selected, or second, the number and/or diameter of primary holes could be reduced so that ϕ_{pz} increases and consequently increases $SMD_{1bo,start}$. A similar procedure is used for the main nozzle, either including or ignoring the contribution from the pilot at idle.

Evaluation of Design Methodology

Using an earlier form of the emissions characteristic time model, Mellor[16] proposed two modified versions of the GT-309 vehicular gas turbine combustor, Mod A and Mod B, which would exhibit reduced NO_x emissions. The geometries of the standard, A, and B combustors are shown in Fig. 7. All three combustors have the same overall length (26.54 cm) and diameter (19.05 cm), have the same dome flow area and configuration, burn the same fuel (DF-2), and have no air swirler. Combustors A and B were rig-tested by Hammond[17] along with the standard GT-309 for the prescribed engine operating cycle shown in Table 2.

With the measured emissions test data for the standard burner and a slight variation on Mellor's model, Hammond correlated NO_x *EI* and CO *EI* with the appropriate characteristic time ratios. The NO_x emissions for modifications A and B were predicted to within one standard deviation for all power conditions, whereas the CO emissions were less accurate. In an attempt to improve on this result, predictions of NO_x and CO emissions were repeated using the current form of the emissions correlations[6] and compared to Hammond's measurements. It is this form of the model on which the design methodology of the previous section is based in part and therefore, satisfactory performance of the model would provide partial methodology validation.

Combustors A and B were designed with the sole intention of reducing NO_x emissions and without any consideration given to flame stabilization. Hammond found that A and B could not sustain stable combustion at low power (corresponding to 50% and 60% of design gasifier speed). Therefore, in addition to investigating CO and NO_x emissions, an effort is conducted to predict Hammond's flame stabilization results for the three combustors using the lean blowoff submodel of the design methodology, the need for which was established by Hammond's findings. These results are presented in the section which follows.

The NO_x model used in the present study differs from that used by Hammond in some important ways. First, the activation energies *E* shown in Fig. 2 are slightly different. Second, different methods for evaluating the primary zone airflow split are used. Finally, the present model uses a slope and intercept based on a correlation involving three different engines including the GT-309, while Hammond's NO_x (and CO) predictions are based on a correlation of the GT-309 only. The present CO model also differs from that used by Hammond in

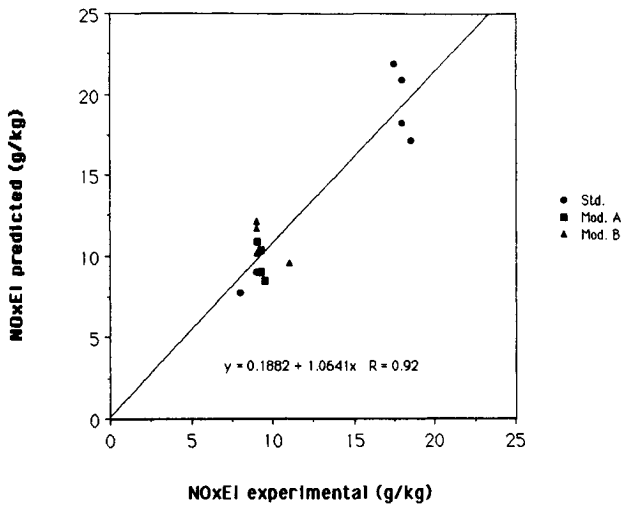

Fig. 8 NO_x *EI* predicted vs measured values using current version of model.

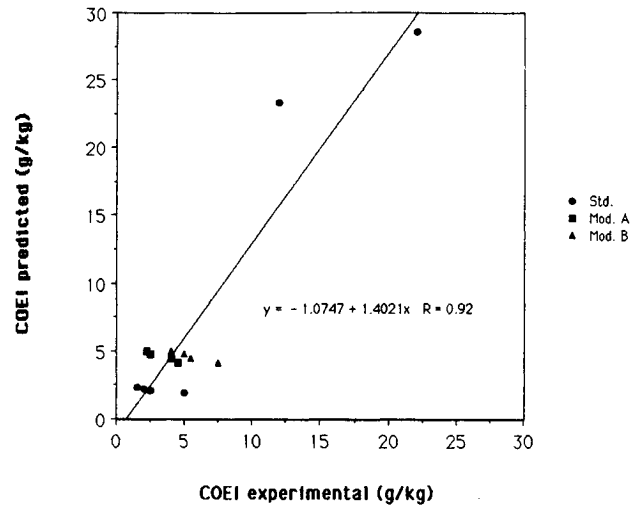

Fig. 9 CO *EI* predicted vs measured values using current version of model.

that different equations are used to compute τ_{co} and $\tau_{sl,co}$ and different criteria are followed to determine l_{quench}. The present model[6] equates l_{quench} in the l_{co} equation with the air addition site where the local value of ϕ first drops below 0.2, whereas Hammond selected locations that would maximize the overall correlation coefficient.

The NO_x predictions using the present form of the model and measurements for the standard, A, and B combustors are presented in Fig. 8 as NO_x *EI* predicted vs NO_x *EI* experimental (from Hammond's combustor tests). Shown are a total of 14 data points representing the three combustors at the operating points where each sustained stable combustion. The standard GT-309 was stable at all six cycle points, whereas Mod A and Mod B were stable only at the four points which made up the high-power regime (70–100% of design gasifier speed). Thus, only the standard data show variation along the least-squares fit in Fig. 8 as percent of gasifier speed varies from idle at the left to near design and design on the right. The best-fit line for the data for all three combustors has a slope of 1.06 with a negligible intercept term and a correlation coefficient of 0.92. The somewhat low correlation coefficient results from scatter in the model predictions, for example in the near and design power levels for the standard burner (in the upper right of the figure). Scatter is typically ± 3 g NO_x/kg fuel, based on the three engine correlation of Mellor and Washam.[6]

A similar best-fit line of NO_x *EI* data from Hammond's correlation equation (derived from Mellor's 1977 model) vs NO_x *EI* experimental for the standard, A, and B combustors has a slope of 0.93, a negligible intercept term, and a correlation coefficient of 0.94. Since both best-fit lines have slopes equally close to an ideal value of 1.00, small y intercepts, and near-equal values of R, the correlation coefficient, it is concluded that the two NO_x models are equivalent.

The CO results for the present model are presented in Fig. 9 as CO *EI* predicted vs CO *EI* experimental (from Hammond's combustor tests). As the figure shows, the best-fit line through the 14 data points has a slope of 1.40, an intercept of -1.07, and a correlation coefficient of 0.92. The CO *EI* data from Hammond's correlation equation vs CO *EI* experimental have a best-fit line with a slope of 0.87, an intercept of $+1.83$, and an R value of 0.94. Since this line has a slope closer to the ideal value of 1.00 and has a higher correlation coefficient, one concludes that the earlier form of the CO model performs somewhat better than the present form.

However, neither the CO nor NO_x results with the current emissions models demonstrate significantly worsened predictions. As these more general forms represent correlations of data from three widely differing combustors, they are significant improvements over those by Mellor[16] and used by Hammond,[17] and thus allow design of low-emissions configurations with considerably more confidence.

Use of Design Methodology in Combustor Design

The design methodology is used in this section to design a modification of the GT-309 vehicular gas turbine combustor that will not only meet the emissions goals of the previous section but also exhibit stable combustion at idle. This modification is designated "Mod C." Combustors A and B were shown in the previous section to exhibit the predicted reductions in NO_x but increases in CO emissions when compared to the standard GT-309 combustor.[17] Mod C is designed using the current characteristic time model therefore to exhibit a 50% reduction in NO_x *EI* at full power *without* an increase in CO *EI* at idle. This emissions goal eventually leads to the specification of primary and secondary hole locations, numbers, and diameters.

Other restrictions placed on Mod C include a combustion efficiency at idle no less than 99% and a blowout fuel–air ratio no greater than the fuel–air ratio at the 50% power condition. Ignition performance is not considered due to a lack of information about the spark energy and start requirements. With the above information established, the fuel injector used in the standard GT-309 is either accepted or rejected for use in Mod C.

Some simplifying assumptions about Mod C are made before the methodology is implemented. Mod C and the standard combustor are alike in the following ways: both combustor liners have the same overall length (26.54 cm), diameter (19.05 cm), and total area occupied by air addition apertures (108.58 cm^2). Both combustors have the same dome flow area and configuration, are subjected to the same prescribed operating conditions, burn the same fuel type (DF-2), and have no air swirler.

Hammond[17] reported that the standard GT-309 combustor yielded a NO_x *EI* value of approximately 18 g NO_2/kg fuel at full power during rig testing. Therefore, in order to achieve the desired 50% reduction in NO_x *EI* at full power for Mod C, a NO_x *EI* value of 9 g NO_2/kg fuel is specified to the NO_x algorithm along with inlet conditions at 100% of design gasifier speed. Tentative choices of $d_{sec} = 3$ cm and $n_{sec} = 10$ are made. Following the method outlined in Fig. 2 for obtaining l_{sec} yields a value of 6.41 cm. Since this secondary length is less than the overall length of Mod C (26.54 cm), a change in neither d_{sec} nor n_{sec} is required.

As mentioned earlier, Mod C is to produce no increase in CO emissions at idle over the standard GT-309. Hammond[17]

found that the standard combustor yielded a CO *EI* of approximately 22 g CO/kg fuel at idle. This CO *EI* value is used in the CO algorithm along with inlet conditions at 50% of design gasifier speed. A value for l_{pri} equal to 3.64 cm is obtained as output.

Since this primary length is less than the secondary length and the difference in lengths ($l_{sec} - l_{pri}$) seems reasonable, no change in the preliminary design is obvious at this point. However, when the diameter and number of primary holes are determined, there is not enough primary zone area available for primary holes due to the relatively large ratio of secondary hole area to total hole area. In other words, the area occupied by primary holes, equal to ($A_{pz} - A_{dome}$), is a negative value. The solution to this problem involves decreasing d_{sec} and/or n_{sec} in order to allot more of the total hole area for the primary zone [thus making ($A_{pz} - A_{dome}$) positive]. Keeping d_{sec} fixed at 3 cm and decreasing n_{sec} from 10 to 8 yields a secondary length equal to 7.96 cm. This design change produces the desired result; an area of 8.2 cm^2 is created for primary holes.

Choosing 10 primary holes for this design sets the hole diameter at 1.0 cm. The location of these holes, however, causes interference with the film-cooling slots. The upstream or leading edge of the primary holes (at a downstream distance of 3.14 cm from the injector) overlaps the film-cooling slots (where $l_{film} = 3.4$ cm; see Fig. 7). Following Mellor,[16] l_{pri} is moved downstream to allow 1.0 cm between the slot exit and the upstream edge of the 1.0 cm diam primary holes. This places the primary holes at $l_{pri} = 4.9$ cm. This 1.3 cm increase in l_{pri} (from 3.6 to 4.9 cm) will yield slightly lower CO *EI* predictions.

The design features of Mod C specified by the methodology at this point are summarized: $l_{sec} = 8.0$ cm, $d_{sec} = 3.0$ cm, $n_{sec} = 8$; and $l_{pri} = 4.9$ cm, $d_{pri} = 1.0$ cm, $n_{pri} = 10$. This liner configuration allows approximately 48% of the inlet airflow to be introduced into the combustor's primary zone compared to approximately 42% in the case of the standard GT-309; the two burners are compared in Fig. 10.

At this point a preliminary design for Mod C has been established with the exception of an atomizer. For the purpose of this exercise, the atomizer used in Hammond's combustor testing is again chosen for use in Mod C. Using the design methodology, this combustor-atomizer configuration is examined to discover whether it meets the efficiency and blowout requirements. Recall that the combustion efficiency at idle must be no less than 99% and that the combustor should not become unstable above the fuel-air ratio at the 50% power condition. These restrictions along with inlet conditions at 50% of design and fuel properties of DF-2 are inputed to the efficiency and lean blowoff algorithms yielding maximum allowable SMD's of 84 μm and 114 μm, respectively. These SMD values are obtained from Eq. (4) once values for τ_{eb} and β are determined. However, β is a function of SMD via the Nusselt number *Nu* in its convective correction (see Leonard and Mellor[9] and Peters and Mellor[11]). Thus, an iteration is established between the final SMD's required for the efficiency and blowout goals and the chosen SMD's in the *Nu* equation. Eventually, *Nu* was calculated for 115 μm which yielded the 114 μm lean blowoff value and for 85 μm which yielded the 84 μm efficiency value. These chosen SMD's, if then held constant in the *Nu* equation, predict combustion efficiencies and lean blowoff fuel-air ratios shown in Fig. 11 for Mod C.

The single orifice, pintle type, air assist atomizer chosen for Mod C produces a spray of DF-1 at ambient temperature and pressure with an SMD at idle fuel flow equal to 33 μm according to Hammond.[18] Since the SMD operating with DF-2 in the primary zone at engine conditions is unknown, we assume 33 μm for the latter as well. Therefore, the Mod C combustor-atomizer configuration satisfies both the efficiency and flame-stability goals. This result is demonstrated graphically in Fig. 11 which shows that for a 33-μm mean droplet diameter fuel spray, the combustion efficiency is approximately 99.5% and the blowout fuel-air ratio is about six times less than the fuel-air ratio at 50% of design.

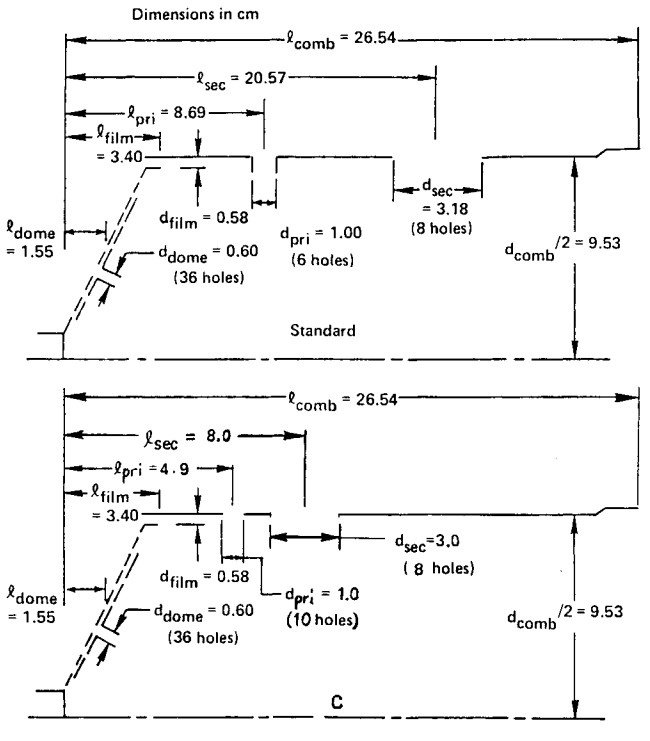

Fig. 10 Geometries for standard and modification C GT-309 combustors.

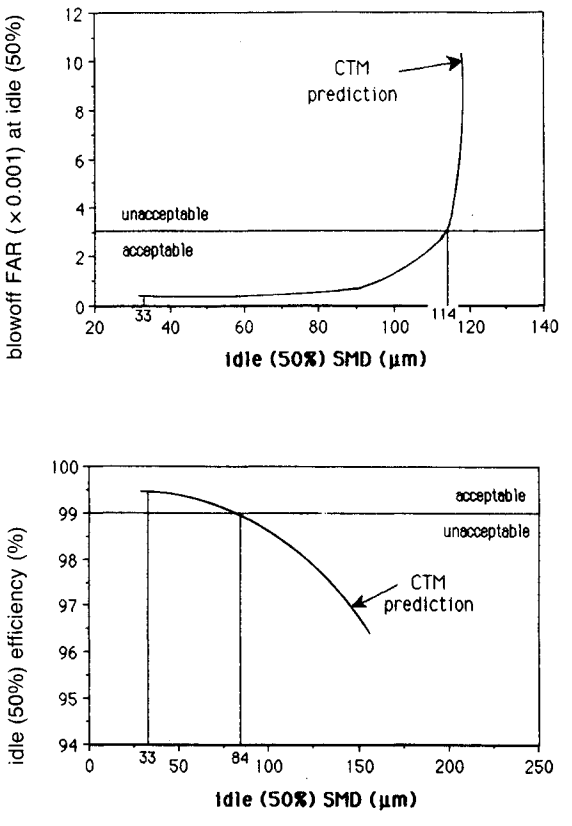

Fig. 11 Blowoff fuel/air ratio and combustion efficiency at 50% power for modification C using current versions of model (CTM).

Table 3 Lean blowoff characteristic times at 50% power

Combustor modification	τ_{sl}, ms	τ_{hc}, ms	τ_{eb}, ms	$(\tau'_{hc} + 0.011\ \tau'_{eb})$[a], ms
Standard	1.96	0.034	2.09	0.178
A and B	1.51	0.116	2.09	0.434
C	1.28	0.037	2.09	0.187

[a]Taking SMD on DF-2 at engine idle as 33 μm, basing ϕ_{pz} on a design value of 0.8 for the standard burner at 100% power (Cornelius and Wade[19]), and including multiplication by $T_{\phi=1}/T_{in}$ which is denoted by the primes.

As another test of the lean blowoff model, the equation in Fig. 6 is used to examine flame stabilization at 50% power for all four GT-309 combustors. Recall that from rig tests, the standard combustor was stable at 50% while Mod A and Mod B were not, and from the design methodology, Mod C is expected to be stable at 50%. Slope m_{lbo} in the correlation is not specified because its value 1.36 was derived for the AGT-1500, T-63, and J85 combustors, and not the GT-309.

Table 3 shows the characteristic times at 50% power for all four burners. Since lean blowoff characteristic times for Mod A and Mod B are calculated to be equivalent, both combustors are considered as one category in the table. The last column shows right-hand side values of the blowoff criterion without the slope and intercept terms. The τ_{sl} reveal a decreasing trend moving from the standard to Mod C which is caused by changes in combustor geometry only, since the power condition remains constant at 50%. Specifically, the decreasing trend is due to a decrease in the downstream location of each combustor's primary air addition holes as shown in Figs. 7 and 10. Since τ_{eb} is evaluated with 33 μm for all four combustors, its value remains constant. Finally, for combustors A and B, τ_{hc} is more than three times greater than the near-equal τ_{hc} for the standard and Mod C.

Because power condition is held constant at 50%, τ_{hc} for lean blowoff is inversely proportional to primary zone equivalence ratio. Therefore, from Table 3, Mod A and Mod B are significantly leaner at 50% than the standard and Mod C, as expected since A and B have one row of relatively large holes which add large amounts of air to the primary zone. This lean situation, therefore, can promote or cause lean blowout to occur for A and B at 50% as it did for Hammond during rig testing. Mod C, however, has a richer primary zone than A and B since it has two rows of holes like the standard, evident in the near-equal τ_{hc} (and ϕ_{pz}) for the standard and Mod C combustors.

Flame-stabilization expectations for all four combustors are summarized in Fig. 12, which shows qualitatively where each combustor should fall with respect to the stability limit line (of slope "m" and intercept "b") at 50%. Given that τ_{sl} is fixed by combustor geometry and τ'_{eb} is constant, one can hypothesize that the relatively high τ_{hc} for A and B is driving those combustors into the unstable region of Fig. 12, while the lower τ_{hc} values for the standard and Mod C are keeping them in the stable region.

Our goal therefore is to determine what values of "m" and "b" produce the qualitative situation presented in Fig. 12 using the data of Table 3. Table 4 shows left-hand side (LHS) and right-hand side (RHS) values, where τ_{sl} (LHS) must be greater than or equal to $[m(\tau'_{hc} + 0.011\ \tau'_{eb}) + b]$ (RHS) in order for a combustor to exhibit combustion stability, for three combinations of m and b. The first combination has $m = 1.36$ and $b = 0.36$ as in Derr and Mellor,[15] determined in a correlation effort involving the AGT-1500, T-63, and J85, and predicts A and B to be stable (since LHS > RHS) which contradicts experimental results. The second combination of m and b retains the slope of 1.36 but uses the standard deviation in the lean blowoff data from Derr and Mellor[15] of ± 0.4 to increase b from 0.36 to 0.76, but still predicts that A and B are stable at 50%. However, any value of m between 2.0 and 3.5 times the recommended value of 1.36 will give a

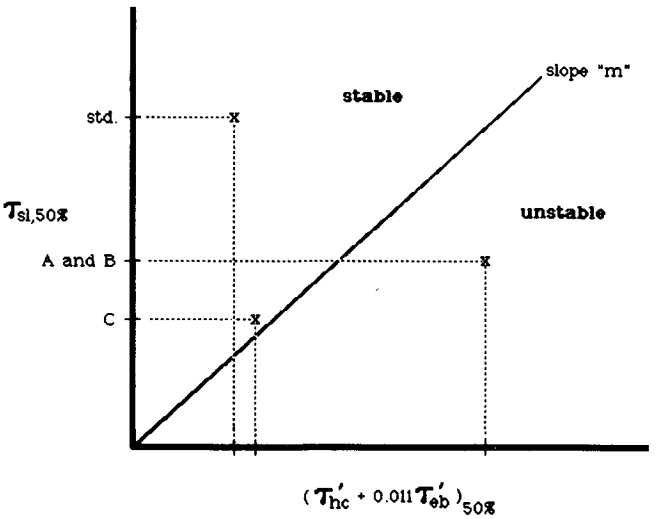

Fig. 12 Qualitative stability map in terms of characteristic times showing expected operating points for the four GT-309 burners at 50% power.

Table 4 Left- and right-hand side values (in ms) of blowoff limit equation various values of "m" and "b"

Combustor modification	$m = 1.36$ and $b = 0.36$		$m = 1.36$ and $b = 0.76$		$m = 3.00$ and $b = 0.36$	
	LHS	RHS	LHS	RHS	LHS	RHS
Standard	1.96	0.60	1.96	1.00	1.96	0.89
A and B	1.51	0.95	1.51	1.35	1.51	1.66
C	1.28	0.62	1.28	1.02	1.28	0.92

quantitatively accurate position for the line in Fig. 12: the case for $m = 3.00$ and $b = 0.36$ is shown in the final column of Table 4.

Therefore, Derr and Mellor's[15] slope and standard deviation do not accurately predict lean blowoff for Mod A and Mod B because, apparently, the stability limit for the four versions of the GT-309 does not fall on the same line as the AGT-1500, T-63, and J85. However, because no lean limit data, specifically fuel-air ratio at blowoff, are available for the standard GT-309 or Mod A or Mod B, a refinement to the model equation cannot be made to accurately predict lean blowoff for the GT-309-class combustors.

The point is addressed in the work of Cornelius and Wade,[19] who tested seven geometries in addition to the standard GT-309. Their early quench, Mod 2 burner has a configuration closest to the present Mod C, but smaller l_{pri}, larger l_{sec}, and a richer primary zone (see Mellor[16]). NO_x data at 50 and 60% power are listed for this burner,[19] indicating stable operation at both power levels.

Another issue raised by the data for the early quench, Mod 2 combustor is CO emissions, generally 2–4 times larger than those for the standard burner,[16] whereas recall Mod C was designed allowing no increase in CO. The major difficulty in the CO *EI* model is the location of the CO quench length.[17] In the design methodology, this position is always taken as l_{pri}, even though criteria for its location have been developed (e.g., Mellor and Washam,[6] and Leonard[8]). This decision was a result of the need to uncouple the primary penetration hole design from the other outputs of the methodology, and should be expected to lead to inaccurate estimates of CO emissions. Nevertheless, we feel the approach outlined here has merit.

Conclusions

A systematic combustor design procedure, based on quantitative performance goals of NO_x, CO, combustion efficiency, and lean lightoff and blowoff limits, is proposed. Outputs

from the model include number, size, and position of primary and secondary air penetration jets and fuel spray SMD's at start and engine idle. GT-309 combustor modifications are designed using current forms of the characteristic time model, and design predictions for two of the modifications, for which rig data exist, are reasonably accurate. The final design is expected to exhibit satisfactory combustion efficiencies and blowoff limits at low powers. Further applications of the methodology in the design process will improve its utility.

Acknowledgments

The work reported here was supported in part by Allison Gas Turbine Division, GMC (PO H723417) with N. K. Rizk and H. C. Mongia as technical monitors, and by the National Science Foundation (Grant ENG-8712997) with R. Rostenbach as monitor. W. S. Derr of Drexel University also provided considerable assistance.

References

[1]Dodds, W. J., and Ekstedt, E. E., "Broad Specification Fuels Combustion Technology Program, Phase 1," NASA CR-168179, 1984.

[2]Mellor, A. M., "Semiempirical Correlations for Gas Turbine Emissions, Ignition, and Flame Stabilization," *Progress in Energy Combustion Science,* Vol. 6, No. 4, 1980, pp. 347-358.

[3]Lefebvre, A. H., "Influence of Fuel Properties on Gas Turbine Combustion Performance," Air Force Wright Aeronautical Lab., Wright-Patterson AFB, OH, AFWAL-TR-84-2104, 1985.

[4]Rizk, N. K., and Mongia, H. C., "Gas Turbine Combustor Design Methodology," AIAA Paper 86-1531, 1986.

[5]Mongia, H. C., "A Status Report on Gas Turbine Combustion Modeling," Paper 26, AGARD CP 422, *Combustion and Fuels in Gas Turbine Engines,* 1987.

[6]Mellor, A. M., and Washam, R. M., "Characteristic Time Correlations of Pollutant Emissions from an Annular Gas Turbine Combustor," *AIAA Journal of Energy,* Vol. 3, July-Aug. 1979, pp. 250-253.

[7]Lefebvre, A. H., "Fuel Effects on Gas Turbine Combustion," Air Force Wright Aeronautical Lab., Wright-Patterson AFB, OH, AFWAL-TR-83-2004, 1983.

[8]Leonard, P. A., "Correlation of the Effects of Fuel Type on Gas Turbine Combustor Efficiency," Ph.D. Thesis, School of Mechanical Engineering, Purdue Univ. West Lafayette, IN, 1981.

[9]Leonard, P. A., and Mellor, A. M., "Correlation of Gas Turbine Efficiency," *AIAA Journal of Energy,* Vol. 7, Nov.-Dec. 1983, pp. 596-602.

[10]Godsave, G. A. E., "Studies of the Combustion of Drops in a Fuel Spray—The Burning of Single Drops of Fuel," *Fourth Symposium (International) on Combustion,* Williams and Wilkins, Baltimore, MD, 1953, pp. 818-830.

[11]Peters, J. E., and Mellor, A. M., "A Spark Ignition Model for Liquid Fuel Sprays Applied to Gas Turbine Engines," *AIAA Journal of Energy,* Vol. 6, July-Aug. 1982, pp. 272-274.

[12]Jarymowycz, T. A., and Mellor, A. M., "Effects of Alternative Fuels on Ignition Limits of the J85 Annular Combustor," *AIAA Journal of Propulsion and Power,* Vol. 3, May-June 1987, pp. 283-288.

[13]Moses, C. A. et al., "Development of an Alternative Test Procedure to Qualify Fuels for Navy Aircraft," Naval Air Propulsion Test Center, NAPC-PE-145C, 1984.

[14]Peters, J. E., and Mellor, A. M., "Characteristic Time Ignition Model Extended to an Annular Gas Turbine Combustor," *AIAA Journal of Energy,* Vol. 6, Nov.-Dec. 1982, pp. 439-441.

[15]Derr, W. S., and Mellor, A. M., "Characteristic Times for Lean Blowoff in Turbine Combustors," *AIAA Journal of Propulsion and Power,* Vol. 3, No. 4, July-Aug. 1987, pp. 377-380.

[16]Mellor, A. M., "Characteristic Time Emissions Correlation and Sample Optimization: GT-309 Gas Turbine Combustor," *AIAA Journal of Energy,* Vol. 1, No. 4, July-Aug. 1977, pp. 244-249.

[17]Hammond, D. C., Jr., "Evaluating Characteristic Time Emissions Predictions for Three Vehicular Gas Turbine Combustors," *AIAA Journal of Energy,* Vol. 1, July-Aug. 1977, pp. 250-256.

[18]Hammond, D. C., Jr., private communication, General Motors Research Lab., 1988.

[19]Cornelius, W., and Wade, W. R., "Emissium Characteristics of Continuous Combustion Systems of Vehicular Powerplants—Gas Turbine, Steam, Stirling," *Emissions from Continuous Combustion Systems,* Plenum, New York, 1972, pp. 375-450.